JACS
JOURNAL OF THE AMERICAN CHEMICAL SOCIETY
ARTICLE
pubs.acs.org/JACS

Photocatalytic Reduction of Carbon Dioxide over Ag Cocatalyst-Loaded $ALa_4Ti_4O_{15}$ (A = Ca, Sr, and Ba) Using Water as a Reducing Reagent

Kosuke Iizuka,[†] Tomoaki Wato,[†] Yugo Miseki,[†] Kenji Saito,[†,‡] and Akihiko Kudo*[,†,‡]

[†]Department of Applied Chemistry, Faculty of Science, and [‡]Division of Photocatalyst for Energy and Environment, Research Institute of Science and Technology, Tokyo University of Science, 1-3 Kagurazaka, Shinjuku-ku, Tokyo 162-8601, Japan

S Supporting Information

ABSTRACT: Ag cocatalyst-loaded $ALa_4Ti_4O_{15}$ (A = Ca, Sr, and Ba) photocatalysts with 3.79−3.85 eV of band gaps and layered perovskite structures showed activities for CO_2 reduction to form CO and HCOOH by bubbling CO_2 gas into the aqueous suspension of the photocatalyst powder without any sacrificial reagents. Ag cocatalyst-loaded $BaLa_4Ti_4O_{15}$ was the most active photocatalyst. A liquid-phase chemical reduction method was better than impregnation and in situ photodeposition methods for the loading of the Ag cocatalyst. The Ag cocatalyst prepared by the liquid-phase chemical reduction method was loaded as fine particles with the size smaller than 10 nm on the edge of the $BaLa_4Ti_4O_{15}$ photocatalyst powder with a plate shape during the CO_2 reduction. CO was the main reduction product rather than H_2 even in an aqueous medium on the optimized $Ag/BaLa_4Ti_4O_{15}$ photocatalyst. Evolution of O_2 in a stoichiometric ratio (H_2+CO:O_2 = 2:1 in a molar ratio) indicated that water was consumed as a reducing reagent (an electron donor) for the CO_2 reduction. Thus, an uphill reaction of CO_2 reduction accompanied with water oxidation was achieved using the $Ag/BaLa_4Ti_4O_{15}$ photocatalyst.

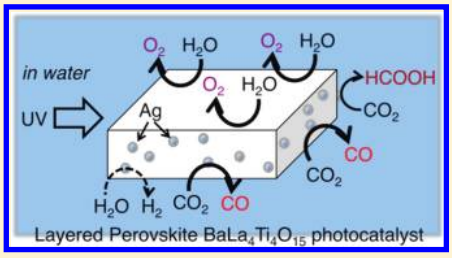

INTRODUCTION

CO_2 reduction to produce usable products is an important topic from the viewpoint of not only an environmental issue but also artificial photosynthesis. If one thinks artificial photosynthesis accompanied by light energy conversion, water has to be used as an electron donor and a hydrogen source for the CO_2 reduction. A photocatalytic system is a candidate for the CO_2 reduction of an artificial photosynthesis in an aqueous medium as well as an electrochemical system combined with a solar cell. The photocatalytic reduction of CO_2[1] has been studied for a long time as well as water splitting.[2,3] When homogeneous photocatalysts such as an Re complex are used, CO_2 is efficiently reduced to form CO in the presence of electron donors such as triethanol amine.[4−7] However, water cannot be used as an electron donor for the CO_2 reduction accompanied by O_2 evolution because of the lack of ability of water oxidation. Heterogeneous photocatalysts have also been studied. It has been reported that TiO_2 and $SrTiO_3$ photocatalysts give HCOOH, HCHO, CH_3OH, and CH_4, depending on cocatalysts loaded on the photocatalysts.[8−31] Various hydrocarbons are also detected using a mesoporous TiO_2 photocatalyst.[22] Mixed metal oxides such as $CaFe_2O_4$,[32,33] $LaCoO_3$,[34] $BiVO_4$,[35] $InTaO_4$,[36] $ZnGa_2O_4$,[37] and Zn_2GeO_4[38,39] have also been reported as nontitanate photocatalysts. However, the amounts of products are small, and O_2 is not determined even in the absence of a sacrificial reagent in many cases. Moreover, contaminations adsorbed on photocatalysts sometimes give carbon-containing products.[31] On the other hand, colloidal ZnS[40,41] and CdS[42,43] photocatalysts show the activities for CO_2 reduction to form HCOOH and CO with high quantum yields. Especially, the CdS photocatalyst works under visible light irradiation. However, electron donors such as triethylamine and 2-propanol are indispensable for suppression of photocorrosion for these metal sulfide photocatalysts. In contrast, when a UV-responsive ZrO_2 photocatalyst with 5 eV of a band gap is employed, CO and H_2 simultaneously evolve accompanied by O_2 evolution in an aqueous medium without electron donors.[44] The selectivity for the CO formation was about 10% when a Cu cocatalyst was loaded on the photocatalyst, indicating the major reaction was still H_2 evolution by reduction of H_2O. It is a challenging theme to develop highly efficient photocatalysts for CO_2 reduction using water as an electron donor.

We have reported various d^0-type metal oxide photocatalysts with wide band gaps for water splitting into H_2 and O_2.[2] Electrons photogenerated in conduction bands of these photocatalysts possess high reducing potentials. Therefore, these photocatalysts are expected to be active also for CO_2 reduction using water as a reducing reagent, if a suitable reaction site for CO_2 reduction is introduced as a cocatalyst on the surface of a photocatalyst. $ALa_4Ti_4O_{15}$ (A = Ca, Sr, and Ba) photocatalysts with layered perovskite structure show high activities for water splitting.[45] These photocatalyst powders prepared by a polymerizable complex method possess plate shape reflecting the crystal structure.

Received: August 11, 2011
Published: November 16, 2011

Table 1. CO_2 Reduction over $ALa_4Ti_4O_{15}$ (A = Ca, Sr, and Ba) Photocatalysts with Various Cocatalysts[a]

photocatalyst	band gap/eV	cocatalyst (wt %)	loading method	activity/μmol h^{-1}			
				H_2	O_2	CO	HCOOH
$BaLa_4Ti_4O_{15}$	3.9	none		5.3	2.4	0	0
$BaLa_4Ti_4O_{15}$	3.9	NiO_x[b] (0.5)	impregnation	58	29	0.02	0
$BaLa_4Ti_4O_{15}$	3.9	Ru (0.5)	photodeposition	84	41	0	0
$BaLa_4Ti_4O_{15}$	3.9	Cu (0.5)	photodeposition	96	45	0.6	0
$BaLa_4Ti_4O_{15}$	3.9	Au (0.5)	photodeposition	110	51	0	0
$BaLa_4Ti_4O_{15}$	3.9	Ag (1.0)	photodeposition	10[c]	7.0[c]	4.3[c]	0.3[c]
$CaLa_4Ti_4O_{15}$	3.9	none		1.3	0.6	0.07	0
$CaLa_4Ti_4O_{15}$	3.9	Ag (1.0)	photodeposition	5.6	2.1	2.3	1.3
$SrLa_4Ti_4O_{15}$	3.8	none		0.8	0.5	0.06	0
$SrLa_4Ti_4O_{15}$	3.8	Ag (1.0)	photodeposition	2.7	1.8	1.8	0.5

[a] Catalyst 0.3 g, water 360 mL, CO_2 flow system (15 mL min^{-1}), a 400 W high-pressure mercury lamp, an inner irradiation quartz cell. [b] Pretreatment: Reduced at 673 K and subsequently oxidized at 473 K after impregnation (543 K for 1 h). [c] Initial activity.

The anisotropic property of $BaLa_4Ti_4O_{15}$ is stronger than those of $SrLa_4Ti_4O_{15}$ and $CaLa_4Ti_4O_{15}$ because of the ordered distribution of alkali earth metal and lanthanum cations in the layered perovskite structure of $BaLa_4Ti_4O_{15}$.[46] The reduction site is the edge of the plate, while the oxidation site is the basal plane. These separated reaction sites are convenient to suppression of back reactions for photocatalytic reactions.

In the present study, we employed the $ALa_4Ti_4O_{15}$ (A = Ca, Sr, and Ba) photocatalysts loaded with various cocatalysts for CO_2 reduction using water as a reducing reagent. Factors affecting the activity were discussed on the basis of the examination and characterization of cocatalysts.

RESULTS AND DISCUSSION

Photocatalytic Reduction of CO_2. Table 1 shows effects of cocatalyst, the loading method, and the loading amount on CO_2 reduction in aqueous media over $ALa_4Ti_4O_{15}$ (A = Ca, Sr, and Ba) photocatalysts. Bare $ALa_4Ti_4O_{15}$ (A = Ca, Sr, and Ba) showed negligible activities for CO_2 reduction. Loading pretreated NiO, Ru, and Au cocatalysts on $BaLa_4Ti_4O_{15}$ enhanced photocatalytic activity for water splitting, but not CO_2 reduction, because these cocatalysts are highly effective for H_2 production by water splitting.[47,48] When a Cu cocatalyst was loaded, photocatalytic activities for water splitting and CO_2 reduction increased. Although the amounts of reacted electrons and holes were large in the order of Au > Cu > Ru > NiO_x > Ag, Ag was the most active cocatalyst for CO_2 reduction. Reduction of CO_2 to form CO and HCOOH competed with that of water to form H_2. The Ag cocatalyst was also effective for CO_2 reduction over $CaLa_4Ti_4O_{15}$ and $SrLa_4Ti_4O_{15}$ photocatalysts. It has been reported that Ag is a highly active electrocatalyst for electrochemical reduction of CO_2 to form CO selectively in an aqueous $KHCO_3$ solution as shown in eq 1.[49,50]

$$CO_2 + 2H^+ + 2e^- \rightarrow CO + H_2O \quad (1)$$

This fact indicated that the Ag cocatalyst functioned as a CO_2 reduction site to form CO. The amount of HCOOH formed was small, because Ag was not a suitable cocatalyst for it. Moreover, HCOOH should not accumulate in a liquid phase because it is readily oxidized by photogenerated holes. This was confirmed experimentally as shown in Figure S1. When a bare $BaLa_4Ti_4O_{15}$ photocatalyst was irradiated with UV in an aqueous HCOOH solution, reduction of water proceeded accompanied by sacrificial consumption of HCOOH, in addition to decomposition of HCOOH to form CO.

Particle size and condition of the Ag cocatalyst depend on the loading method and should affect the photocatalytic activity. Therefore, the loading method and amounts on $ALa_4Ti_4O_{15}$ (A = Ca, Sr, and Ba) photocatalysts were examined for the photocatalytic CO_2 reduction (Table 2). These Ag-loaded $ALa_4Ti_4O_{15}$ (A = Ca, Sr, and Ba) photocatalysts showed activities for CO_2 reduction to form CO and HCOOH. The photocatalytic activity of $BaLa_4Ti_4O_{15}$ with the Ag cocatalyst loaded by an impregnation method was improved by H_2 reduction at 473 K for 2 h. A liquid-phase chemical reduction was the best loading method for the Ag cocatalyst. CO_2 reduction to form CO and HCOOH was superior to H_2O reduction to form H_2. This method was more effective than a photodeposition method also for $CaLa_4Ti_4O_{15}$ and $SrLa_4Ti_4O_{15}$ photocatalysts, as shown in Table 1.

The reduction of CO_2 predominantly proceeded at any loading amounts of the Ag cocatalyst on $BaLa_4Ti_4O_{15}$. The optimum amount of the Ag cocatalyst was 2 wt %. Photocatalytic CO_2 reduction over the optimized Ag/$BaLa_4Ti_4O_{15}$ is shown in Figure 1. CO, H_2, and O_2 evolved with stoichiometric amounts. The ratio of the number of reacted electrons to that of holes was almost unity. Turnover numbers of electrons reacted for CO_2 reduction to the number of moles of total Ag and surface Ag were 5.5 and 75 at 7 h, respectively. These results indicated that the CO_2 reduction photocatalytically proceeded. The $ALa_4Ti_4O_{15}$ (A = Ca, Sr, and Ba) photocatalysts were calcined at 1373 K in air during the preparation. No C−H stretching peak around 2900 cm^{-1} was observed by IR measurement. When Ar was flowed instead of CO_2, water splitting proceeded to form H_2 and O_2 without carbon-contained products as shown in Table 2. These results have proven that the formed CO and HCOOH were originated from not contaminations but CO_2. This is also supported by unity of the ratio of reacted e^-/h^+. Thus, it was found that Ag cocatalyst-loaded $ALa_4Ti_4O_{15}$ (A = Ca, Sr, and Ba) was the photocatalyst for CO_2 reduction to form CO using water as an electron donor.

Characterization of Ag-Loaded $BaLa_4Ti_4O_{15}$ Photocatalyst. Diffuse reflectance spectra of $BaLa_4Ti_4O_{15}$ with Ag cocatalysts loaded by various methods are shown in Figure 2 to see the condition of metallic Ag loaded. The absorption with an onset at 320 nm was due to the band gap transition of $BaLa_4Ti_4O_{15}$.

Table 2. Effect of Loading Method of Ag Cocatalyst on the Photocatalytic Activity for CO_2 Reduction over $ALa_4Ti_4O_{15}$ (A = Ca, Sr, and Ba)[a]

photocatalyst	loading amount/wt %	loading method	activity/μmol h^{-1}			
			H_2	O_2	CO	HCOOH
$BaLa_4Ti_4O_{15}$	1.0	impregnation[b]	8.2	5.7	5.2	0.2
$BaLa_4Ti_4O_{15}$	1.0	impregnation[b]+H_2 red.[c]	5.6	8.7	8.9	0.3
$BaLa_4Ti_4O_{15}$	0.5	liquid-phase reduction	4.5	6.8	11	0.03
$BaLa_4Ti_4O_{15}$	1.0	liquid-phase reduction	5.6	12	19	0.4
$BaLa_4Ti_4O_{15}$	2.0	liquid-phase reduction	10	16	22	0.7
$BaLa_4Ti_4O_{15}$	3.0	liquid-phase reduction	9.7	14	19	0.1
$BaLa_4Ti_4O_{15}$	5.0	liquid-phase reduction	4.8	6.6	12	0.02
$BaLa_4Ti_4O_{15}$	1.0	liquid-phase reduction	20[d]	11[d]	0[d]	0[d]
$SrLa_4Ti_4O_{15}$	1.0	liquid-phase reduction	4.8	5.8	7.1	0.8
$CaLa_4Ti_4O_{15}$	1.0	liquid-phase reduction	3.2	6.6	9.3	0.4

[a] Catalyst 0.3 g, water 360 mL, CO_2 flow system (15 mL min^{-1}), a 400 W high-pressure mercury lamp, an inner irradiation quartz cell. [b] 723 K for 1 h. [c] 473 K for 2 h. [d] Ar flow.

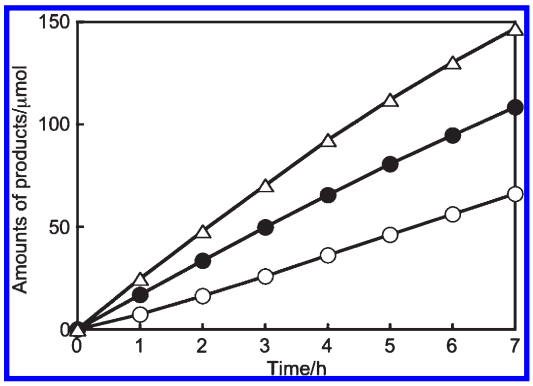

Figure 1. CO_2 reduction over $BaLa_4Ti_4O_{15}$ photocatalyst with Ag (2 wt %) cocatalyst loaded by a liquid-phase reduction method. Catalyst 0.3 g, water 360 mL, CO_2 flow system (15 mL min^{-1}), a 400 W high-pressure mercury lamp, an inner irradiation quartz cell, H_2 (○), O_2 (●), CO (△).

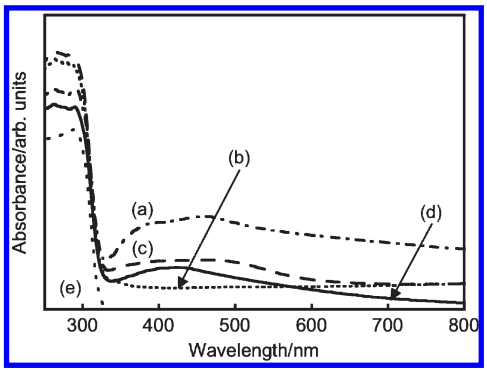

Figure 2. Diffuse reflection spectra over $BaLa_4Ti_4O_{15}$ photocatalyst with Ag (1 wt %) cocatalyst loaded by (a) photodeposition, (b) impregnation, (c) impregnation+H_2 reduction, (d) liquid-phase reduction, and (e) bare $BaLa_4Ti_4O_{15}$.

A surface plasmon absorption around 400−500 nm and a wide absorption band continuing to a near-infrared region due to large particles of metallic Ag were observed in the case of photodeposition. The surface plasmon absorption was not observed for the Ag cocatalyst loaded by an impregnation method, suggesting the existence of silver oxide on the cocatalyst surface, whereas it was observed after H_2 reduction of the sample. A simple profile of the surface plasmon absorption and small absorption due to the large particle of metallic Ag were observed for the Ag cocatalyst loaded by a liquid-phase chemical reduction, indicating Ag cocatalysts were loaded as fine metallic particles with a size with a relatively narrow distribution.

Figure 3 shows SEM images of Ag cocatalyst-loaded $BaLa_4Ti_4O_{15}$ photocatalysts. $BaLa_4Ti_4O_{15}$ had a plate shape with 100 nm thickness and 1 μm width reflecting a layered perovskite structure. Photodeposited Ag cocatalysts in situ were loaded on the edge of the plate as nanoparticles with the size of 30−40 nm. The particle size of photodeposited Ag in situ after 1 h of the photocatalytic reaction was similar to that after 7 h. Ag cocatalysts loaded by an impregnation method and subsequent H_2 reduction aggregated with the size of 50 nm. Ag cocatalysts prepared by a liquid-phase chemical reduction were uniformly and dispersively loaded on the $BaLa_4Ti_4O_{15}$ photocatalyst with the size smaller than 10 nm. The Ag cocatalyst on the basal plane of $BaLa_4Ti_4O_{15}$ almost disappeared, and the number of the Ag particles on the edge increased even after 1 h of the photocatalytic reaction. It has been reported that reduction by photogenerated electrons and oxidation by holes proceed mainly on the edge and basal plane for water splitting on $BaLa_4Ti_4O_{15}$, respectively.[45] This anisotropic property has been clarified by reductive photodeposition of Au and oxidative photodeposition of PbO_2 being similar to TiO_2.[5,51] This result suggested that the Ag on the basal plane dissolved by photogenerated holes and photodeposited again on the edge at the initial stage of the photocatalytic reaction. The size of rephotodeposited Ag on the edge was smaller than 10 nm and more uniform than photodeposited Ag of Figure 3a. The reason the size of the rephotodeposited Ag on the edge shown in Figure 3g was smaller than the just photodeposited Ag shown in Figure 3a is due to the rate of photodeposition. The concentration of dissolved Ag^+ ions in an aqueous solution for the rephotodeposited sample was lower than that for the just photodeposited sample. Absorption band due to surface plasmon after the reaction still possessed a simple profile with a peak shape as shown in Figure 4, being different from that in Figure 2a. This result also indicated that the nature of the Ag cocatalyst loaded

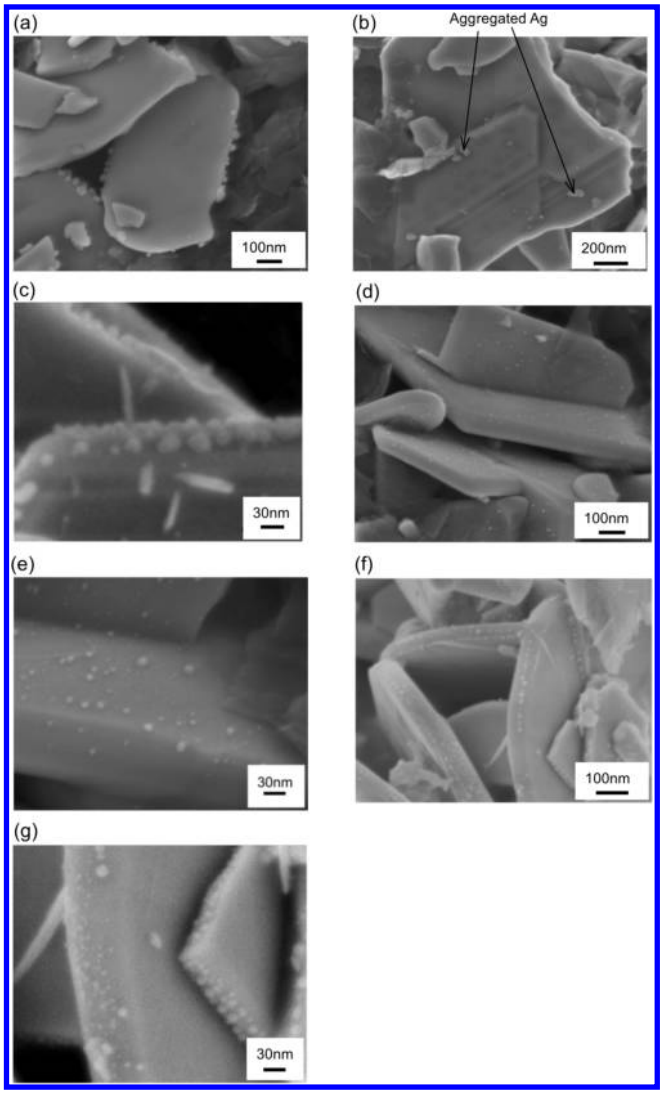

Figure 3. Scanning electron microscope images of Ag (1 wt %)/$BaLa_4Ti_4O_{15}$. (a) Photodeposition, (b) impregnation+H_2 reduction (as prepared), (c) impregnation+H_2 reduction (after photocatalytic CO_2 reduction for 1 h), (d) liquid-phase reduction (as prepared), (e) magnified view of (d), (f) liquid-phase reduction (after photocatalytic CO_2 reduction for 1 h), and (g) magnified view of (f).

by a liquid-phase chemical reduction, subsequent photodissolution, and rephotodeposition during the photocatalytic reaction was different from that loaded by photodeposition in situ. The difference in the photocatalytic activity between photodeposition and liquid-phase reduction was due to the difference in the size and homogeneity of loaded Ag cocatalysts even if the cocatalysts were photodeposited on the edge under the working state. Although the shape of the surface plasmon band after CO_2 reduction was similar to that before the reaction, the intensity after the reaction was larger than that before the reaction, suggesting that the number of the metallic Ag fine particle increased. The rephotodeposition was also seen in the case of samples with impregnation+H_2 reduction as shown in Figure 3c. The size of Ag rephotodeposited on the edge was 10−20 nm. Therefore, the order in the size of Ag cocatalyst under working condition was liquid-phase reduction < impregnation and H_2 reduction < photodeposition, corresponding to the order in the

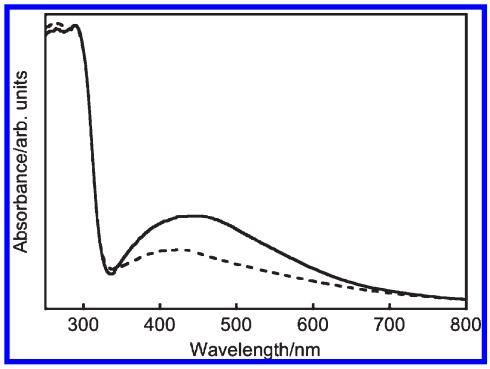

Figure 4. (a) Diffuse reflection spectra of Ag (1 wt %)/$BaLa_4Ti_4O_{15}$ before (− − −) and after (−) CO_2 reduction reaction.

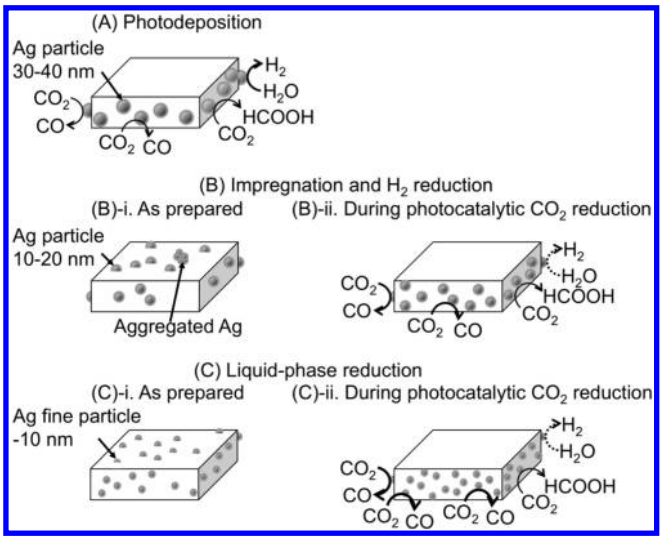

Figure 5. Mechanism of photocatalytic CO_2 reduction over $BaLa_4Ti_4O_{15}$ with Ag cocatalysts loaded by several methods.

catalytic activity for CO_2 reduction. These results indicated that the critical factor contributing to facilitate CO/HCOOH evolution was particle size of Ag loaded on the edge of a $BaLa_4Ti_4O_{15}$ crystal. XPS measurements indicated that the metallic state of Ag was maintained even after 20 h of photocatalytic reaction (Figure S2).[S2] The stability of metallic state of Ag resulted from the loading position, that is, edges of a $BaLa_4Ti_4O_{15}$ crystal, which acted as reduction sites.

Scheme of Photocatalytic Reduction of CO_2 on Ag/$BaLa_4Ti_4O_{15}$. The scheme of photocatalytic reduction of CO_2 on Ag/$BaLa_4Ti_4O_{15}$ is illustrated in Figure 5. The edge of a $BaLa_4Ti_4O_{15}$ photocatalyst is the reduction site, while the basal plane is the oxidation site for water splitting. This property is due to anisotropy of the crystal structure.[45] The degree of the anisotropy of $BaLa_4Ti_4O_{15}$ is larger than those of $SrLa_4Ti_4O_{15}$ and $CaLa_4Ti_4O_{15}$ due to distribution of the alkali earth metal cations in layered perovskite structure. The most active $BaLa_4Ti_4O_{15}$ photocatalyst with fine Ag cocatalysts loaded on the edge under working state possesses the ideal structure for the photocatalytic CO_2 reduction. CO_2 reduction proceeds on the Ag cocatalyst loaded on the edge competing with H_2O reduction, while O_2 evolution mainly proceeds on the basal plane. The CO_2 reduction to form CO predominated over the H_2O reduction to give

H_2 on the $BaLa_4Ti_4O_{15}$ photocatalyst with Ag cocatalysts loaded by liquid-phase reduction and impregnation+H_2 reduction, whereas it was reverse for photodeposition as shown in Tables 1 and 2. The separation of the reaction sites contributes to suppression of back reactions such as oxidation of formed CO. The reactions were carried out under CO_2 flow. The bubbling of CO_2 also assists to get the gaseous products out into a gas phase, resulting in the suppression of back reactions. Moreover, the photocatalytic reaction may proceed at the three-phase interface among the surface of photocatalyst, liquid of water, and a gas phase. When CO_2 gas was flowed on an aqueous suspension of the photocatalyst without bubbling, the photoctalytic activity was considerably decreased as compared to the bubbling system (Figure S3), suggesting that the photocatalytic reaction proceeded at the three-phase interface.

CONCLUSIONS

$BaLa_4Ti_4O_{15}$ with anisotropic structure showed higher photocatalytic activity for CO_2 reduction than $SrLa_4Ti_4O_{15}$ and $CaLa_4Ti_4O_{15}$. The ratio of the number of reacted electrons to holes was unity, indicating that water reacted as an electron donor. Ag was the most active cocatalyst. The Ag cocatalyst functioned as a CO_2 reduction site to form CO as seen in an Ag electrocatalyst for electrochemical reduction of CO_2. The photocatalytic activity depended on the loading method of the Ag cocatalyst. The liquid-phase chemical reduction was the best method to load fine Ag particles, and the condition of the Ag cocatalyst changed at the beginning stage of the photocatalytic reaction. CO mainly evolved on the Ag cocatalyst loaded on the edge of plate particle of the $BaLa_4Ti_4O_{15}$ photocatalyst. High activity of Ag/$BaLa_4Ti_4O_{15}$ for the photocatalytic CO_2 reduction using water is due to separated reaction sites of reduction from oxidation, and specific loading of the Ag cocatalyst on the edge. Moreover, a CO_2 bubbling method contributed to suppressing of back reactions and serving the three-phase interface for the reaction.

EXPERIMENTAL SECTION

$ALa_4Ti_4O_{15}$ (A = Ca, Sr, and Ba) photocatalysts were prepared by a polymerizable complex method.[45] Ethanol suspension containing titanium-*n*-butoxide (Kanto chemical, 97.0%), citric acid (Kanto chemical, 99.5%), and propylene glycol (Kanto chemical, 99.0%) was stirred at 333 K. After complete dissolution of the citric acid, lanthanum nitrate (Wako, 99.9%) and alkaline earth carbonates ($CaCO_3$, Kanto chemical, 99.5%; $SrCO_3$, Kanto chemical, 99.9%; $BaCO_3$, Kanto chemical, 99.5%) were added to this solution, and the mixture was heated at 393 K for 12 h to afford gel assembly. The gel was thermally decomposed at 673 K in air, followed by calcination at 1373 K for 10 h to obtain photocatalyst powder.

Ru, Cu, and Au cocatalysts were loaded on photocatalysts by a photodeposition in situ from aqueous solutions dissolving $RuCl_3$, $CuSO_4$, and $HAuCl_4$. A NiO cocatalyst was loaded by an impregnation method in which water was evaporated from the suspension of the photocatalyst in an aqueous $Ni(NO_3)_2$ solution on a water bath and the resulting solid was calcined at 543 K. The photocatalyst powder loaded with NiO was reduced by H_2 gas at 673 K for 2 h and subsequently oxidized by O_2 gas at 473 K for 1 h after the impregnation as pretreatment. An Ag cocatalyst was loaded on the photocatalyst by photodeposition, impregnation, and liquid-phase chemical reduction methods using $AgNO_3$. Photodeposition was conducted in situ at the beginning stage of a photocatalytic reaction. An aqueous $AgNO_3$ solution and calcination at 723 K for 1 h were selected as the condition of the impregnation method. Reduction treatment was performed under H_2 gas flow at 473 K for 2 h if needed. In the liquid-phase chemical reduction method,[53−55] an aqueous $AgNO_3$ solution (0.1 mol/L) was added to 50 mL of an aqueous suspension containing 0.5 g of the photocatalyst. After addition of an equimolar amount of $NaPH_2O_{2aq}$ (0.4 mol/L) with respect to Ag^+ to the suspension, the mixture was stirred at 333 K for 1 h. The obtained powder was washed with water and dried at ambient temperature in air.

The photocatalysts obtained were identified by powder X-ray diffraction (Rigaku; Miniflex, Cu Kα). Diffuse reflection spectra were recorded on a UV−vis−NIR spectrometer (JASCO; UbestV-570) and were converted from reflection to absorbance by the Kubelka−Munk method. Scanning electron microscopy (SEM) images were taken using a JEOL JSM-6700F.

CO_2 gas with a purity of 99.995% was used. This gas contained a negligible amount of CO as compared to the amounts of produced CO shown in Tables 1 and 2. 0.3 g of the photocatalyst powder was dispersed in 360 mL of water. Photocatalytic reactions were carried out by bubbling the CO_2 gas with a flow rate at 15 mL min^{-1} using an inner irradiation cell made of quartz and a 400 W high-pressure mercury lamp (a spectrum of incident light, see Figure S4) under ambient temperature and pressure. Gaseous products of H_2, O_2, and CO were determined by online gas chromatographs (Shimadzu, GC-8A) with a thermal conductivity detector (MS-5A, Ar carrier) and a flame ionization detector (MS-13X, N_2 carrier) with a methanizer. An aqueous product of formic acid was analyzed by an ion chromatograph (TOA-DKK, ICA-2000, DS-plus).

ASSOCIATED CONTENT

Supporting Information. Decomposition of HCOOH over a bare $BaLa_4Ti_4O_{15}$ photocatalyst in an aqueous medium (S1), Ag($M_4N_{4,5}N_{4,5}$) Auger spectra of $BaLa_4Ti_4O_{15}$ photocatalyst loaded with Ag (2 wt %) by a liquid-phase chemical reduction method before and after 20 h of photocatalytic reaction (S2), photocatalytic CO_2 reduction over Ag(2 wt %)/$BaLa_4Ti_4O_{15}$ with and without bubbling CO_2 gas (S3), and a spectrum of incident light from a light source of a 400 W high-pressure mercury lamp + a quartz cell (S4). This material is available free of charge via the Internet at http://pubs.acs.org.

AUTHOR INFORMATION

Corresponding Author
a-kudo@rs.kagu.tus.ac.jp

ACKNOWLEDGMENT

This work was supported by the ENEOS hydrogen foundation.

REFERENCES

(1) Roy, S. C.; Varghese, O. K.; Paulose, M.; Grimes, C. A. *ACS Nano* **2010**, *4*, 1259.
(2) Kudo, A.; Miseki, Y. *Chem. Soc. Rev.* **2009**, *38*, 253.
(3) Osterloh, E. F. *Chem. Mater.* **2008**, *20*, 35.
(4) Takeda, H.; Ishitani, O. *Coord. Chem. Rev.* **2010**, *254*, 346.
(5) Grills, D. C.; Fujita, E. *J. Phys. Chem. Lett.* **2010**, *1*, 2709.
(6) Takeda, H.; Koike, K.; Inoue, H.; Ishitani, O. *J. Am. Chem. Soc.* **2008**, *130*, 2023.
(7) Hawecker, J.; Lehn, J.-M.; Ziessel, R. *Helv. Chim. Acta* **1986**, *69*, 1990.
(8) Inoue, T.; Fujishima, A.; Konishi, S.; Honda, K. *Nature* **1979**, *209*, 101.
(9) Halmann, M.; Ulman, M.; Aurian-Blajeni, B. *Solar Energy* **1983**, *31*, 429.

(10) Tennakone, K. *Solar Energy Mater.* **1984**, *10*, 235.
(11) Halmann, M.; Katzir, V.; Borgarello, E.; Kiwi, J. *Solar Energy Mater.* **1984**, *10*, 85.
(12) Ishitani, O.; Inoue, C.; Suzuki, Y.; Ibusuki, T. *J. Photochem. Photobiol., A: Chem.* **1993**, *72*, 269.
(13) Solymosi, F.; Tombácz, I. *Catal. Lett.* **1994**, *27*, 61.
(14) Willner, I.; Heleg, V. *J. Chem. Soc., Chem. Commun.* **1994**, 2113.
(15) Mizuno, T.; Adachi, K.; Ohta, K.; Saji, A. *J. Photochem. Photobiol., A: Chem.* **1996**, *98*, 87.
(16) Anpo, M.; Yamashita, H.; Ichihashi, Y.; Fujii, Y.; Honda, M. *J. Phys. Chem. B* **1997**, *101*, 2632.
(17) Wada, Y.; Ogata, T.; Hiranaga, K.; Yasuda, H.; Kitamura, T.; Murakoshi, K.; Yanagida, S. *J. Chem. Soc., Perkin Trans.* **1998**, *2*, 1999.
(18) Ikeue, K.; Yamashita, H.; Anpo, M.; Takewaki, T. *J. Phys. Chem. B* **2001**, *105*, 8350.
(19) Tseng, I.-H.; Wu, J. C. S.; Chou, H.-Y. *J. Catal.* **2004**, *221*, 432.
(20) Nasution, S.; Purnama, H. W.; Purnama, E.; Kosela, S.; Gunlazuardi, J. *Catal. Commun.* **2005**, *6*, 313.
(21) Xia, X.-H.; Jia, Z.-H.; Yu, Y.; Liang, Y.; Wang, Z.; Ma, L.-L. *Carbon* **2007**, *45*, 717.
(22) Varghese, O. K.; Paulose, M.; LaTempa, T. J.; Grimes, C. A. *Nano Lett.* **2009**, *9*, 731.
(23) Wu, J. C. S. *Catal. Surv. Asia* **2009**, *13*, 30.
(24) Yang, H.-C.; Lin, H.-Y.; Chien, Y.-S.; Wu, J. C. S.; Wu, H.-H. *Catal. Lett.* **2009**, *131*, 381.
(25) Zhao, Z.; Fan, J.; Liu, S.; Wang, Z. *Chem. Eng. J.* **2009**, *151*, 134.
(26) Zhang, Q.-H.; Han, W.-D.; Hong, Y.-J.; Yu, J.-G. *Catal. Today* **2009**, *148*, 335.
(27) Woolerton, T. W.; Sheard, S.; Reisner, E.; Pierce, E.; Ragsdale, S. W.; Armstrong, F. A. *J. Am. Chem. Soc.* **2010**, *132*, 2132.
(28) Koci, K.; Mateju, K.; Obalova, L.; Krejcikova, S.; Lancy, Z.; Placha, D.; Capek, L.; Hospodkova, A.; Solcova, O. *Appl. Catal., B: Environ.* **2010**, *96*, 239.
(29) Li, Y.; Wang, W.-N.; Zhan, Z.; Woo, M.-H.; Wu, C.-Y.; Biswas, P. *Appl. Catal., B: Environ.* **2010**, *100*, 386.
(30) Wang, C.; Thompson, R. L.; Baltrus, J.; Matranga, C. *J. Phys. Chem. Lett.* **2010**, *1*, 48.
(31) Yui, T.; Kan, A.; Saitoh, C.; Koike, K.; Ibusuki, T.; Ishitani, O. *ACS Appl. Mater. Interfaces* **2011**, *3*, 2594.
(32) Matsumoto, Y.; Obata, M.; Hombo, J. *J. Phys. Chem.* **1994**, *98*, 2950.
(33) Matsumoto, Y. *J. Solid State Chem.* **1996**, *126*, 227.
(34) Jia, L.; Li, J.; Fang, W. *Catal. Commun.* **2009**, *11*, 87.
(35) Liu, Y.; Huang, B.; Dai, Y.; Zhang, X.; Qin, X.; Jiang, M.; Whangbo, M.-H. *Catal. Commun.* **2009**, *11*, 210.
(36) Pang, P.-W.; Chen, Y.-W. *Catal. Commun.* **2007**, *8*, 1546.
(37) Yan, S. C.; Ouyang, S. X.; Gao, J.; Yang, M.; Feng, J. Y.; Fan, X. X.; Wan, L. J.; Li, Z. S.; Ye, J.; Zhou, Y.; Zou, Z. G. *Angew. Chem., Int. Ed.* **2010**, *49*, 6400.
(38) Liu, Q.; Zhou, Y.; Kou, J.; Chen, X.; Tian, Z.; Gao, J.; Yang, S.; Zou, Z. *J. Am. Chem. Soc.* **2010**, *132*, 14385.
(39) Zhang, N.; Ouyang, S.; Zhang, Y.; Xi, G.; Kako, T.; Ye, J. *Chem. Commun.* **2011**, *47*, 2041.
(40) Henglein, A.; Gutierrez, M. *Ber. Bunsen-Ges. Phys. Chem.* **1983**, *87*, 852.
(41) Fujiwara, H.; Hosokawa, H.; Murakoshi, K.; Wada, Y.; Yanagida, S. *Langmuir* **1998**, *14*, 5154.
(42) Fujiwara, H.; Hosokawa, H.; Murakoshi, K.; Wada, Y.; Yanagida, S.; Okada, T.; Kobayashi, H. *J. Phys. Chem. B* **1997**, *101*, 8270.
(43) Liu, B.-J.; Torimoto, T.; Yoneyama, H. *J. Photochem. Photobiol., A: Chem.* **1998**, *113*, 93.
(44) Sayama, K.; Arakawa, H. *J. Phys. Chem.* **1993**, *97*, 531.
(45) Miseki, Y.; Kato, H.; Kudo, A. *Energy Environ. Sci.* **2009**, *2*, 306.
(46) Vanderah, T. A.; Collins, T. R.; Won-Ng, W.; Roth, R. S.; Farber, L. *J. Alloys Compd.* **2002**, *346*, 116.
(47) Iwase, A.; Kato, H.; Kudo, A. *Catal. Lett.* **2006**, *108*, 7–10.
(48) Domen, K.; Kudo, A.; Onishi, T.; Kosugi, N.; Kuroda, H. *J. Phys. Chem.* **1986**, *90*, 292–295.
(49) Hori, Y.; Wakabe., H.; Tsukamoto, T.; Koga, O. *Electrochim. Acta* **1994**, *39*, 1833.
(50) Azuma, M.; Hashimoto, K.; Hiramoto, M.; Watanabe, M.; Sakata, T. *J. Electrochem. Soc.* **1990**, *137*, 1772.
(51) Ohno, T.; Sarukawa, K.; Matsumura, M. *New J. Chem.* **2002**, *26*, 1167.
(52) Kaushik, V. K. *J. Electron Spectrosc. Relat. Phenom.* **1991**, *56*, 273.
(53) Chen, L. J.; Wan, C. C.; Wang, Y. Y. *J. Colloid Interface Sci.* **2006**, *297*, 143.
(54) Fievet, F.; Lagier, J. P.; Blin, B. *Solid State Ionics* **1989**, *32*, 198.
(55) Takahashi, H.; Sunagawa, Y.; Myagmarjav, S.; Muramatsu, A. *Catal. Surv. Asia* **2005**, *9*, 187.